

# Design and Evaluation of Neural Network-Based Receiver Architectures for Reliable Communication

§ Hüseyin Çevik<sup>\*†</sup>, § Erhan Karakoca<sup>\*</sup>, İbrahim Hökelek<sup>\*‡</sup>, Ali Görçin<sup>\*‡</sup>

<sup>\*</sup> Communications and Signal Processing Research (HİSAR) Lab., TÜBİTAK BİLGE, Kocaeli, Turkey

<sup>†</sup> Department of Electronics and Communication Engineering, Yıldız Technical University, İstanbul, Turkey

<sup>‡</sup> Department of Electronics and Communication Engineering, İstanbul Technical University, İstanbul, Turkey

Emails: {huseyin.cevik, erhan.karakoca, ibrahim.hokelek}@tubitak.gov.tr,  
aligorcin@itu.edu.tr

## Abstract

Neural network-based receivers leverage deep learning to optimize signal detection and decoding, significantly improving bit-error rate (BER) and block-error rate (BLER) in challenging environments. This study evaluates various architectures and compares their BER and BLER performance across different noise levels. Two novel models, the Dual Attention Transformer (DAT) and the Residual Dual Non-Local Attention Network (RDNLA), integrate self-attention and residual learning to enhance signal reconstruction. These models bypass conventional channel estimation and equalization by directly predicting log-likelihood ratios (LLRs) from received signals, with noise variance as an additional input. Simulations show that DAT and RDNLA outperform traditional and other neural receiver models under varying signal-to-noise ratios (SNR), while their computational efficiency supports their feasibility for next-generation communication systems.

## Index Terms

Neural receivers, deep learning, OFDM, bit-error-rate (BER), signal processing, 5G, 6G, TensorFlow, Sionna, transformer networks

Neural receivers are transforming modern wireless communication systems by using deep learning to optimize signal detection and decoding, moving beyond traditional model-based approaches. These systems learn from data instead of relying on explicit mathematical models of channel dynamics or noise, improving performance metrics

§ Hüseyin Çevik and Erhan Karakoca contributed equally to this work.

like bit-error rate (BER) and block-error rate (BLER). They excel in complex environments with high mobility, multi-path fading, and interference, making them ideal for next-generation communication systems.

Neural receivers decode signals by learning directly from data, and various neural network architectures, such as convolutional networks, transformers, and hybrid models, have demonstrated improvements in BER and BLER. For example, DeepRx, a fully convolutional network, performs robustly under varying signal-to-noise ratios (SNRs) [1], while HybridDeepRx integrates traditional signal processing with deep learning to optimize performance in challenging conditions like high-order modulations [2]. Transformer Encoder Networks, such as those used in TransRx-6G-V2X for vehicular communications, enhance soft-decision decoding accuracy by capturing global dependencies with self-attention mechanisms that model long-range dependencies, improving BER performance in high-mobility environments [3], [4]. These advancements position neural receivers as a promising solution for next-generation systems, including 5G and 6G networks, satellite communications, IoT, autonomous vehicles, and wireless sensor networks [1]–[3].

Recent studies further substantiate the potential of neural receiver architectures. For instance, Cammerer et al. [5] and Wiesmair et al. [6] have demonstrated that neural receivers can be implemented in real-time while adhering to standard-compliant requirements in 5G multi-user MIMO scenarios. In parallel, advances in end-to-end learning for OFDM systems [7] have successfully reduced pilot overhead, thereby enhancing spectral efficiency. Deep learning-based channel estimation methods that incorporate belief information [8] and transfer learning strategies for SIMO receivers [9] further improve performance by adapting to realistic channel conditions, as validated by over-the-air experiments [10]. Additionally, interpretability analyses [11] and performance verification frameworks for AI-native transceiver actions [12] provide essential insights into the robustness and operational reliability of these models.

This study compares neural network models for neural receiver tasks, evaluating their BER and BLER performance across different noise levels using the Sionna library. The test results are evaluated and explained to provide insights about the models in order to contribute future research in this field. Also, by combining successful features discovered during tests, two new models are proposed for better accuracy.

#### **Contributions:**

- In this work, we introduce two deep-learning models for neural receivers. These models demonstrate notable improvements in both the Block Error Rate (BLER) and the Bit Error Rate (BER).
- We then explore the architecture of these models, carefully going over each element of their construction. We highlight how each element contributes to feature extraction and learning at the global and local levels that eventually affect BLER.
- Lastly, we made publicly available the source code of our proposed models together with other state-of-the-art implementations. This allows researchers and practitioners to explore, test, and expand upon our findings.

**Notation:** Through this paper  $\mathbf{x}$  and  $\mathbf{X}$ , denote a vector and matrix, respectively.  $\mathcal{CN}(\mu, \sigma^2)$ , identify the probability density function of the complex Gaussian distribution with mean  $\mu$  and  $\sigma^2$  variance.  $\mathbf{I}$  denotes an identity matrix. The element-wise Hadamard product is denoted as  $\odot$  and the convolution operation is given by  $*$ .  ${}^H$  and  ${}^T$  represent complex conjugate Hermitian transpose and transpose operators, respectively.

## I. SYSTEM MODEL AND BACKGROUND

We consider a Single-Input Multiple-Output Orthogonal Frequency Division Multiplexing (OFDM) system with  $N_{BS}$  antennas at the Base Station (BS) and consider uplink transmission. As a channel model, 3GPP Clustered Delay Line is used and it is applied in the frequency domain before being received and processed. Rather than just expressing received OFDM subcarriers, given that the transmitted resource grid is  $\mathbf{X} \in \mathbb{C}^{N_{sub} \times N_{sym}}$  where  $N_{sub}$  is the number of subcarriers and  $N_{sym}$  is the number of symbols in the OFDM system, we denote received resource grids at the receiver of the BS as

$$\mathbf{Y} = \mathbf{H} \odot \mathbf{X} + \mathbf{W}, \quad (1)$$

where  $\mathbf{Y} \in \mathbb{C}^{N_{sub} \times N_{sym} \times N_{BS}}$  is the received resource grid at the BS, containing received symbols across subcarriers, OFDM symbols, and receive antennas.  $\mathbf{H} \in \mathbb{C}^{N_{sub} \times N_{sym} \times N_{BS}}$  is the uplink SIMO channel in the frequency domain. Each element  $H_{k,s}^{(n)}$  represents the channel gain for the  $k$ -th subcarrier and  $s$ -th OFDM symbol at the  $n$ -th BS antenna. Finally,  $\mathbf{W} \sim \mathcal{CN}(\mu, \sigma^2 \mathbf{I})$  is the AWGN noise at the BS.

From that point, after receiving OFDM resource grids, the goal of this study is to estimate the LLR values of received constellation points with Deep Learning techniques. However, before proceeding with DL model, we will give traditional receiver blocks required to estimate LLR values. The UE transmits pilot symbols at specific subcarriers and time slots, forming a pilot resource grid  $\mathbf{X}_p$ . The received pilot signals at the BS are

$$\mathbf{Y}_p = \mathbf{H}_p \odot \mathbf{X}_p + \mathbf{W}_p, \quad (2)$$

and the least squares channel estimate at the pilot locations is given by,

$$\hat{\mathbf{H}}_p = \frac{\mathbf{Y}_p}{\mathbf{X}_p} \quad (3)$$

Since pilots are available only at specific time-frequency positions, the full channel matrix  $\hat{\mathbf{H}}$  is obtained by interpolation over the entire OFDM resource grid using linear interpolation. Following channel estimation, the BS performs LMMSE equalization to mitigate fading and noise. The LMMSE equalization matrix for each subcarrier  $k$  and symbol  $s$  is

$$\mathbf{W}_{k,s}^{\text{LMMSE}} = \left( \hat{\mathbf{H}}_{k,s}^H \hat{\mathbf{H}}_{k,s} + \frac{\sigma^2}{E_s} \mathbf{I} \right)^{-1} \hat{\mathbf{H}}_{k,s}^H, \quad (4)$$

and the equalized resource grid can be written as

$$\hat{\mathbf{X}} = \mathbf{W}^{\text{LMMSE}} \mathbf{Y} \quad (5)$$

where  $\mathbf{W}^{\text{LMMSE}} \in \mathbb{C}^{N_{sub} \times N_{sym} \times N_{BS}}$  is the equalization weight matrix for the entire resource grid and  $\hat{\mathbf{X}} \in \mathbb{C}^{N_{sub} \times N_{sym}}$  is the equalized symbol grid. After equalization, the equalized OFDM symbols are converted into bit-level log-likelihood ratios (LLRs). The LLR for the  $i$ -th bit considering a QAM symbol is computed as:

$$\mathbf{L}_i = \log \frac{P(b_i = 1 | \hat{\mathbf{X}})}{P(b_i = 0 | \hat{\mathbf{X}})} \quad (6)$$

where  $\mathbf{L} \in \mathbb{R}^{N_{sub} \times N_{sym} \times N_{bits}}$  is the LLR grid,  $P(b_i = 1 | \hat{\mathbf{X}})$  and  $P(b_i = 0 | \hat{\mathbf{X}})$  are conditional probability functions for each possible bit values. Finally, the LLRs are fed to the LDPC decoder, which decodes data and reconstructs the transmitted bits.

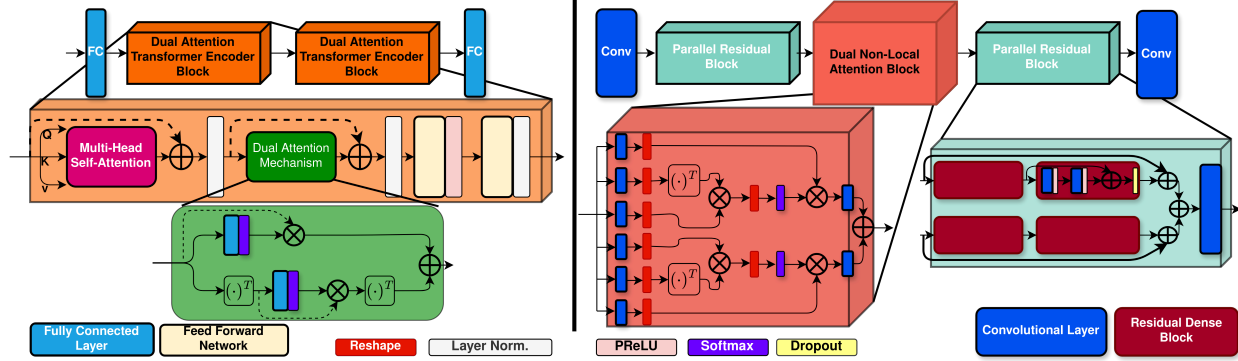


Fig. 1. Caption

## II. PROPOSED DL-BASED LLR ESTIMATION METHODS

In this section, we propose two neural network architectures for directly estimating LLR values from the received OFDM resource grid  $\mathbf{Y}$  (Eq. (1)) [1], [2]. Each network outputs soft-bit log-likelihood ratios  $\mathbf{L}$  (Eq. (6)), bypassing the explicit channel estimation and equalization stages of a conventional receiver [1]. In addition to the received signal samples, noise information in dB is appended as an auxiliary input, enabling the network to leverage the SNR context when producing LLRs.

The received complex-valued OFDM resource grid

$$\mathbf{Y} \in \mathbb{C}^{N_{\text{sub}} \times N_{\text{sym}} \times N_{\text{BS}}},$$

is separated into real and imaginary components, producing a real-valued tensor:

$$\mathbf{Y}_{\text{real}}, \mathbf{Y}_{\text{imag}} \in \mathbb{R}^{N_{\text{sub}} \times N_{\text{sym}} \times N_{\text{BS}}}.$$

We also append the noise variance or SNR (in dB) as an additional “channel” in the input. This can be repeated across the  $(N_{\text{sub}}, N_{\text{sym}})$  grid or broadcast so that each network input token sees the same noise level value. Hence, the overall real-valued input  $\mathbf{x}$  has a shape,

$$\underbrace{(N_{\text{sub}}, N_{\text{sym}}, N_{\text{BS}} \times 2)}_{\text{real+imag}} + 1 \text{ (additional noise term)}, \quad (7)$$

resulting in a total channel dimension of  $2N_{\text{BS}} + 1$ .

### A. Dual Attention Transformer Network

The first architecture is a Dual Attention Transformer (DAT) designed to exploit both spatial (time-frequency) and channel dependencies in the OFDM resource grid. Compared to a standard transformer encoder, DAT incorporates two parallel attention pathways—one focusing on the spatial dimension of tokens, and another focusing on the channel dimension—to improve LLR estimation accuracy.

In Eq. (8)  $\mathbf{x} \in \mathbb{R}^n$  represents the flattened input. Then  $\mathbf{x}$  is mapped to  $T$  tokens of dimension  $d$  with a fully connected (FC) layer as

$$z = \text{FC}(\mathbf{x}) = W\mathbf{x} + \mathbf{b}, \quad z \in \mathbb{R}^{T \times d}, \quad (8)$$

where  $W$  and  $\mathbf{b}$  are learnable parameters, and

$$n = 2N_{\text{sub}}N_{\text{sym}}N_{\text{BS}} + N_{\text{sub}}N_{\text{sym}},$$

if we treat noise dB as an extra channel.

Once tokenized, the data is fed through multiple Dual Attention Transformer Encoder blocks. Each block comprises Multi-Head Self-Attention (MHSA) and a Dual Attention Mechanism (DAM). **First of all**, MHSA captures pairwise correlations among tokens, producing attention-weighted features from  $\mathbf{z}$  by multiplying with three initialized weight matrices to form the query, key, and value matrices,  $\mathbf{Q}$ ,  $\mathbf{K}$ , and  $\mathbf{V}$ , respectively:

$$\mathbf{Q} = zW^Q, \quad \mathbf{K} = zW^K, \quad \mathbf{V} = zW^V. \quad (9)$$

Later, multi-head attention computes the softmax activation and concatenates multiple head outputs, which is then followed by a skip connection and layer normalization.

DAM applies two parallel attention operations—spatial (token-wise) and channel (feature-wise). The computation of these two attentions is given as

$$\mathbf{S} = zW_s \quad \text{and} \quad \mathbf{F}_s = \mathbf{S} \odot z, \quad (10)$$

$$C = z^T W_c \quad \text{and} \quad \mathbf{F}_c = C \odot z^T, \quad (11)$$

respectively, and then sums the results as

$$\mathbf{F}_{\text{dual}} = \mathbf{F}_s + \mathbf{F}_c^T. \quad (12)$$

Another skip connection is added to ensure stable gradients. A two-layer MLP with ReLU nonlinearity further refines the representations. Finally, layer normalization is applied to complete the block. In short, DAT emphasizes learning token-wise (spatial) and feature-wise (channel) correlations via self-attention and dual attention blocks. It is particularly adept at capturing long-range dependencies across subcarriers and symbols.

### B. Residual Dual Non-Local Attention Network

The second architecture, the Residual Dual Non-Local Attention Network (RDNLA), combines convolution-based residual blocks (to capture local and multi-level features) with non-local attention modules (to capture global dependencies). Similar to the DAT, it also employs a dual-attention concept—applying non-local attention both spatial-wise and channel-wise—while explicitly harnessing the noise dB input alongside the real and imaginary resource grid.

Residual Dual Non-Local Attention Network (RDNLA) combines the benefits of residual connections and non-local attention. Residual blocks capture local and multi-level features, while non-local blocks provide global dependency modeling. A “dual” non-local strategy further splits attention into spatial-wise and channel-wise branches.

Firstly, a convolutional layer extracts low-level features as

$$\mathbf{F}_0 = \sigma(W_0 * \mathbf{x} + \mathbf{b}_0), \quad (13)$$

where  $\mathbf{x}$  is the input,  $*$  denotes convolution,  $\sigma(\cdot)$  is an activation function, and  $W_0, b_0$  are the weights and bias. The network then applies a Parallel Residual Block (PRB), which merges features from two parallel “arms,” each containing Residual Dense Blocks (RDBs). Each RDB is defined as

$$\mathbf{F}_{\text{RDB}} = \mathbf{x} + \text{Dropout}(\sigma(W_2 * \sigma(W_1 * \mathbf{x} + b_1) + b_2)). \quad (14)$$

Each arm in the RDB is composed of two sequential RDBs with skip connections around them. The outputs of the two arms are summed and then fused via a convolution, given as

$$A_i = \text{RDB}^{(2)}(\text{RDB}^{(1)}(\mathbf{x})) + \mathbf{x}, \quad i = 1, 2, \quad (15)$$

$$\mathbf{F}_{\text{PRB}} = W_{\text{agg}} * (A_1 + A_2) + b_{\text{agg}}. \quad (16)$$

Then, the output of the PRB is passed to the Dual Non-Local Attention Block (DNLB). A Non-Local Attention layer captures global dependencies by computing pairwise correlations among feature locations. In the dual variant, these non-local operations are applied in parallel over spatial and channel dimensions. **Firstly**,  $1 \times 1$  convolutions are utilized to halve the channel dimension and mix channel information without changing spatial dimensions. This operation is performed by three separate convolutional layers with their own trainable weights. Then, the output of the convolutions is reshaped to obtain tokenized representations. After these operations,  $\theta$ ,  $\phi$ , and  $g$  matrices are obtained. The pairwise attention map is calculated by:

$$A_s = \text{softmax}(\theta(\tilde{x}) \phi(\tilde{x})^T). \quad (17)$$

Then,  $A_s$  and the  $g$  matrix are multiplied to generate the transformed feature matrix to be propagated further:

$$y_s = A_s \cdot g(X).$$

Next, the transformed feature matrix is reshaped back to its original form as the height and width are two separate dimensions. Another convolutional layer is then applied to restore channel dimensions to their original size.

Following that, a similar non-local operation is performed along the channel-wise direction (using a transpose operation that swaps channel and token dimensions), yielding  $\mathbf{y}_c$ . Lastly, the two outputs are summed to obtain the final attention output. A skip connection adds the input  $\mathbf{x}$  back to preserve identity information:

$$\mathbf{F}_{\text{NLA}} = \mathbf{x} + (\mathbf{y}_s + \mathbf{y}_c). \quad (18)$$

Finally, a convolution maps the processed feature maps to LLR values:

$$\mathbf{y}_{\text{LLR}} = W_f * \mathbf{F}_{\text{final}} + b_f, \quad (19)$$

yielding  $\mathbf{L} \in \mathbb{R}^{N_{\text{sub}} \times N_{\text{sym}} \times N_{\text{bits}}}$ .

In summary, RDNLA leverages convolutions and residual dense blocks for strong local and multi-scale feature extraction, while non-local attention captures global dependencies.

### C. Model Training

The given models are trained using the bit-metric decoding (BMD) rate, which serves as an information theoretic objective for bit-interleaved coded modulation (BCIM) systems. The BMD rate is computed from the transmitted coded bits and the predicted LLRs, and its optimization ensures accurate soft-bit estimation for subsequent decoding. BCE loss function compares the predicted LLRs with the true transmitted coded bits over the entire OFDM resource grid, which is given by

$$\mathcal{L}_{\text{BCE}}(B, \hat{L}) = \mathbb{E}[B \log \sigma(\hat{L}) + (1 - B) \log(1 - \sigma(\hat{L}))], \quad (20)$$

where  $B$  represents the transmitted ground truth bits and  $\hat{L}$  represents the predicted LLRs, finally  $\sigma(\hat{L})$  is the sigmoid activation ensuring LLR interpretation as probabilities. In Eq. (20) we used the expectation operator  $\mathbb{E}[\cdot]$  for conciseness, which expresses averaging over all batch examples, subcarriers, OFDM symbols, and bits. The goal of the model is to learn the optimal parameters that minimize the loss function in Eq. (20), formulated as:

$$\theta^* = \arg \min_{\theta} \mathcal{L}_{\text{BCE}}(B, f_{\theta}(\mathbf{Y}, \mathbf{W}_0)), \quad (21)$$

where  $\theta$  represents the learned parameters of the model, and  $f_{\theta}(\cdot)$  is the mapping function, also known as the LLR estimator. The model predicts the LLR values as  $\hat{\mathbf{L}} = f_{\theta}(\mathbf{Y}, \mathbf{W}_0)$ , where  $\mathbf{W}_0$  is noise level, and each element of  $\hat{\mathbf{L}} \in \mathbb{R}^{M \times K \times S \times I}$  corresponds to the LLR of the  $i$ -th coded bit at subcarrier  $k$ , OFDM symbol  $s$ , and batch sample  $m$ . The noise term  $\mathbf{W}_0$  is appended as dB values to the last dimension of  $\mathbf{Y}$  to incorporate noise information during training.

## III. SIMULATION METRICS AND RESULTS

For the system parameters, we consider a UE with a single antenna  $N_{\text{UE}} = 1$  and a BS with two antennas  $N_{\text{BS}} = 2$ , operating in a single stream configuration. The OFDM system consists of 76 subcarriers and 14 OFDM symbols per frame, with 2 symbols allocated for pilots. A cyclic prefix of 6 samples is used to mitigate inter-symbol interference (ISI). The signal is modulated using Quadrature Phase Shift Keying (QPSK), while LDPC encoding and decoding are applied at a coding rate of  $R_C = 0.5$ . The performance simulations given in terms of BER and BLER are evaluated between  $-3$  and  $5$   $E_b/N_0$ (dB). Performance is measured in 3200 Monte-Carlo iterations, with the target block error run set to 1000. For training, we set a batch size of 128 and a total epoch number is 100.000.

The BER versus  $E_b/N_0$  graph distinguishes two groups of receiver architectures above 2 dB. The first group—ResNet, ResDNLA, DA Transformer, Transformer—achieves bit error rates below  $10^{-5}$  before 2 dB. Their success stems from components like ResDNLA's non-local blocks, transformer encoder blocks, and residual connections, which effectively capture complex, global relationships and enhance feature representation for neural receiver tasks.

The second group—EffNetV2, ResUNet, RIDNet, and NAFNet—lags by over 3 dB before reaching similar BER levels. Their underperformance is largely due to reliance on global pooling, which, while effective for semantic segmentation, compromises the preservation of critical features for symbol decisions. Additionally, NAFNet's use of simple gating units in its NAF block is insufficient for modeling the necessary complex relationships.

At 0 dB  $E_b/N_0$ , BERs range from  $1.63 \times 10^{-2}$  to  $6.38 \times 10^{-5}$ . ResDNLA and DA Transformer excel by capturing spatial-channel relationships, while Transformer and residual variants effectively model global dependencies and

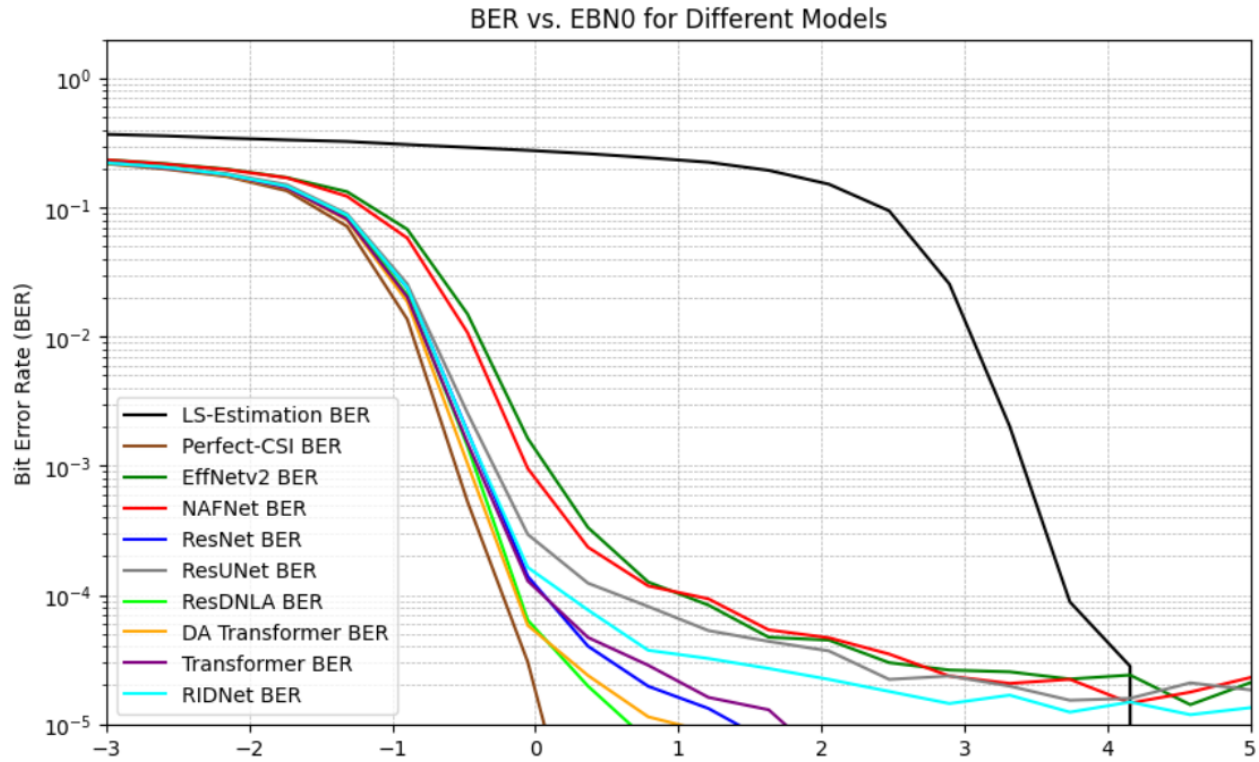


Fig. 2. The neural receiver bit error rate comparison of the proposed neural network models with different noise levels.

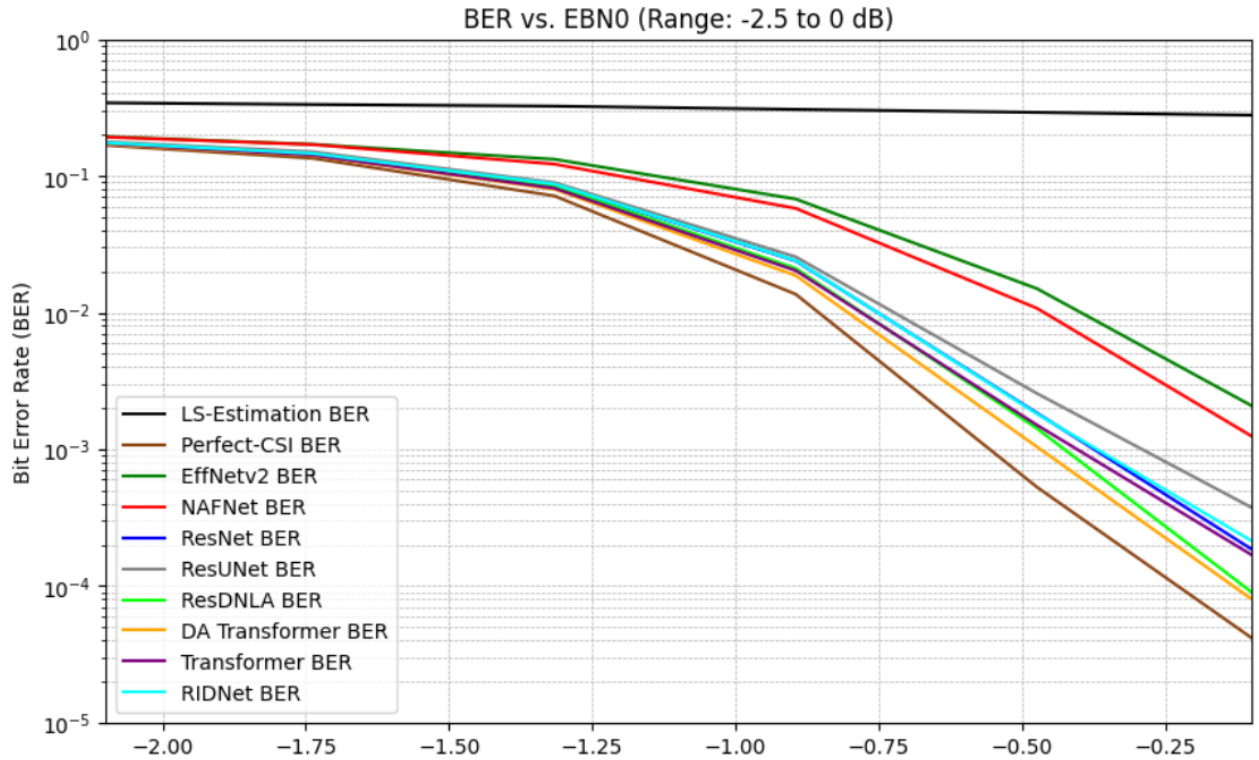


Fig. 3. Bit error rates focused on higher noise levels.

complex features. Additionally, Residual U-Net variants outperform EffNetV2 and NAFNet under these noise conditions.

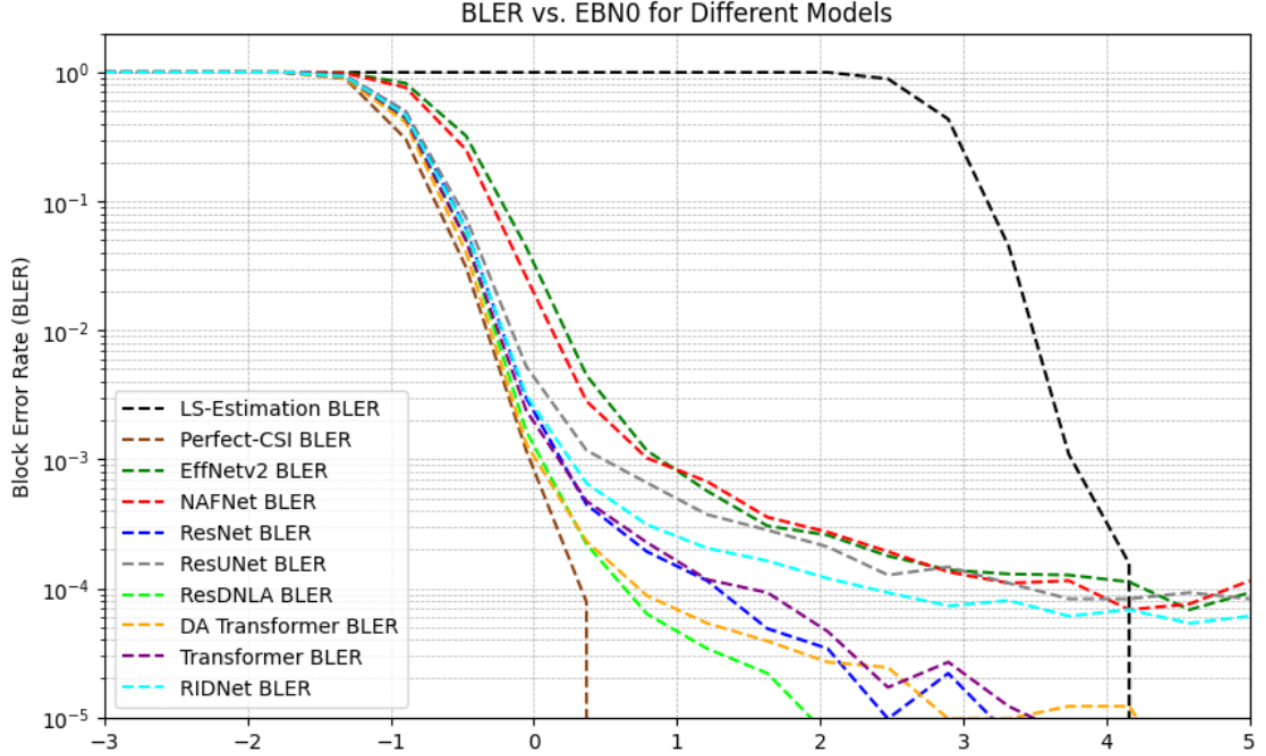


Fig. 4. The neural receiver block error rate comparison of the proposed neural network models with different noise levels.

The BLER graph follows the BER pattern with naturally higher error rates compared to  $E_b/N_0$ , stems from the fact that every bit error is also a block error. We can also see two separated groups mentioned earlier only with an exception. DA Transformer block error rates are struggling to converge at high SNR. This suggests it is more prone to block-level errors, potentially affecting performance dependent on application.

At higher noise levels, block error rates are distributed similarly with bit error rates. Block error rate performances of the models in the same order.

Average computation times are very close as intended. Layer counts and attention mechanism complexities are set to mitigate the computation time difference between various model structures. So, accuracies are more distinctive for the simulation. This condition provides a reference point to measure which model architectures are more suitable for neural receiver tasks.

#### IV. DISCUSSION AND FUTURE WORKS

The results of the BER and BLER evaluations highlight a critical insight: relying solely on Bit Error Rate (BER) does not provide a comprehensive understanding of model performance in communication systems. While BER measures the average number of bit errors, it does not account for the distribution of these errors, which

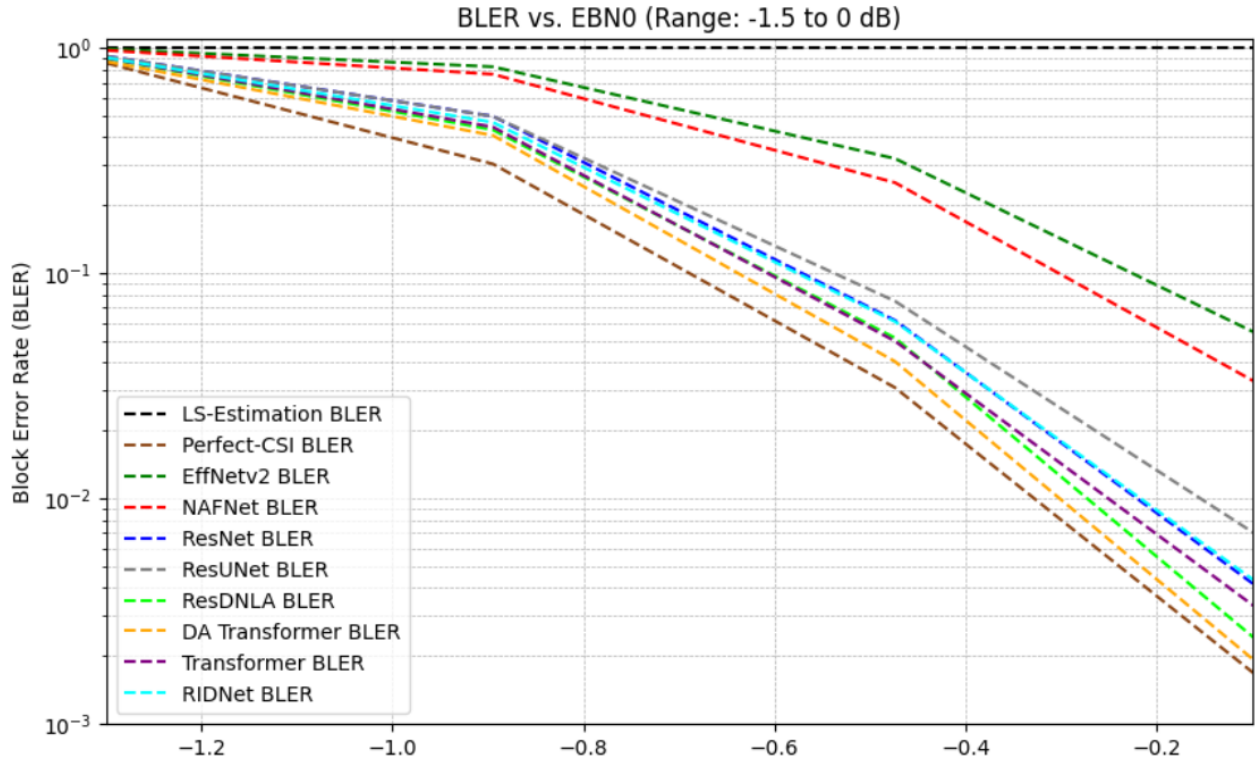


Fig. 5. Block error rates focused on higher noise levels.

TABLE I  
AVERAGE COMPUTATION TIMES OF THE NETWORKS FOR AN OFDM FRAME

| Model                                | Time (milliseconds) |
|--------------------------------------|---------------------|
| EffNet version 2                     | 12.270              |
| NAFNet                               | 11.891              |
| ResNet                               | 12.032              |
| ResUNet (Addition)                   | 12.910              |
| ResDNLNA                             | 12.684              |
| Dual Attention Transformer (Encoder) | 12.366              |
| Transformer (Encoder)                | 11.699              |
| RIDNet                               | 13.349              |

significantly impacts the Block Error Rate (BLER). Our findings indicate that BLER is a more informative metric, as some models exhibit superior BLER performance despite having comparatively higher BER values.

This phenomenon suggests that certain models are more effective at capturing global features of the signal, resulting in scattered individual bit errors rather than consecutive ones. Such error patterns are easier for the decoder to correct, leading to lower BLER. Conversely, other models with lower BER may still yield worse BLER

due to the clustering of errors, which overwhelms the decoder and causes entire blocks to be misinterpreted.

Future work will focus on further analyzing the spatial and temporal distribution of errors to better understand their effect on decoding performance. Additionally, we plan to explore model architectures that explicitly account for error dispersion patterns to optimize BLER performance, potentially incorporating error-aware loss functions or decoder feedback mechanisms during training.

## V. CONCLUSION

Both Dual Attention Transformer and Residual Dual Non-Local Attention architectures aim to learn a direct mapping from the received OFDM signals (plus noise information) to bit-level LLRs. Both proposed networks (DAT and RDNLA) treat the real and imaginary parts of the received OFDM signals, along with noise-level dB, as their primary input. The models can adapt their internal feature extraction and attention mechanisms by integrating noise information to changing SNR conditions. By utilizing self-attention, non-local operations, and residual connections, these networks effectively capture the complex relationships across subcarriers, symbols, and antenna domains, ultimately providing accurate LLR estimates for the subsequent channel decoding.

## REFERENCES

- [1] M. Honkala, D. Korpi, and J. M. Huttunen, “Deeprx: Fully convolutional deep learning receiver,” *IEEE Transactions on Wireless Communications*, vol. 20, pp. 3925–3940, 6 2021.
- [2] J. Pihlajasalo, D. Korpi, M. Honkala, J. M. Huttunen, T. Riihonen, J. Talvitie, A. Brihuega, M. A. Uusitalo, and M. Valkama, “Hybriddeeprx: Deep learning receiver for high-evm signals,” in *IEEE International Symposium on Personal, Indoor and Mobile Radio Communications, PIMRC*, vol. 2021-September. Institute of Electrical and Electronics Engineers Inc., 9 2021, pp. 622–627.
- [3] O. Saleem, S. Ribouh, M. Alfaqawi, A. Bensrhair, and P. Merdignac, “Transrx-6g-v2x : Transformer encoder-based deep neural receiver for next generation of cellular vehicular communications,” 8 2024. [Online]. Available: <http://arxiv.org/abs/2408.01145>
- [4] O. Saleem, M. Alfaqawi, P. Merdignac, A. Bensrhair, and S. Ribouh, “Deep multi-modal neural receiver for 6g vehicular communication,” 1 2025. [Online]. Available: <http://arxiv.org/abs/2501.13464>
- [5] S. Cammerer, F. A. Aoudia, J. Hoydis, A. Oeldemann, A. Roessler, T. Mayer, and A. Keller, “A neural receiver for 5g nr multi-user mimo,” 12 2023. [Online]. Available: <http://arxiv.org/abs/2312.02601>
- [6] R. Wiesmayr, S. Cammerer, F. A. Aoudia, J. Hoydis, J. Zakrzewski, and A. Keller, “Design of a standard-compliant real-time neural receiver for 5g nr,” 9 2024. [Online]. Available: <http://arxiv.org/abs/2409.02912>
- [7] F. A. Aoudia and J. Hoydis, “End-to-end learning for ofdm: From neural receivers to pilotless communication,” *IEEE Transactions on Wireless Communications*, vol. 21, pp. 1049–1063, 2 2022.
- [8] J. Xu, L. Liu, X. Wang, and L. Chen, “Belief information based deep channel estimation for massive mimo systems,” 6 2024. [Online]. Available: <http://arxiv.org/abs/2407.07744>
- [9] U. E. Uyoata and R. O. Adeogun, “On transfer learning for a fully convolutional deep neural simo receiver,” 8 2024. [Online]. Available: <http://arxiv.org/abs/2408.16401>
- [10] R. Luostari, D. Korpi, M. Honkala, and J. M. J. Huttunen, “Adapting to reality: Over-the-air validation of ai-based receivers trained with simulated channels,” 8 2024. [Online]. Available: <http://arxiv.org/abs/2408.04182>
- [11] M. Tuononen, D. Korpi, and V. Hautamäki, “Interpreting deep neural network-based receiver under varying signal-to-noise ratios,” 9 2024. [Online]. Available: <http://arxiv.org/abs/2409.16768>
- [12] N. Soltani, M. Loehning, and K. Chowdhury, “Veritas: Verifying the performance of ai-native transceiver actions in base-stations,” 1 2025. [Online]. Available: <http://arxiv.org/abs/2501.09761>